

Temperature dependent convective parameters for RRc 1D-models

Gábor B. Kovács,^{1,2,3*} János Nuspl,^{2,3} Róbert Szabó^{2,3,4}

¹*ELTE Eötvös Loránd University, Department of Astronomy 1117, Pázmány Péter sétány 1/A, Budapest, Hungary*

²*Konkoly Observatory, Research Centre for Astronomy and Earth Sciences, Eötvös Loránd Research Network (ELKH), MTA Centre of Excellence H-1121 Budapest, Konkoly Thege Miklós út 15-17, Hungary*

³*MTA CSFK Lendület Near-Field Cosmology Research Group, H-1121 Budapest, Konkoly Thege Miklós út 15-17, Hungary*

⁴*ELTE Eötvös Loránd University, Institute of Physics, 1117, Pázmány Péter sétány 1/A, Budapest, Hungary*

Accepted 2023 September 6. Received 2023 August 16; in original form 2023 June 8

ABSTRACT

Nonlinear pulsation modeling of classical variable stars is among the first topics which were developed at the beginning of the computational era. Various developments were made, and many questions were answered in the past 60 years, and the models became more complex, describing the genuinely 3D convection in a single dimension. Despite its successes, the recent public availability of the MESA Radial Stellar Pulsations (MESA RSP) module and the emerging results from multidimensional codes made clear that the 8 free convective parameters, unique to these models, together with the underlying physical models need calibration. This could be done by comparing them against multi-dimensional codes, but before that, it is important to scrutinize the free parameters of the 1D codes using observations. This is a follow-up work of our previous calibration on the convective parameters of the Budapest-Florida and MESA RSP pulsation codes for RRab stars. In this paper, we extend the previous calibration to the RRc stars and the RR Lyrae stars in general. We found that correlations of some of the parameters are present in RRc stars as well but have a different nature, while high-temperature RRc stars' pulsation properties are very sensitive to the chosen parameter sets.

Key words: convection – methods: numerical – stars: oscillations – stars: variables: RR Lyrae — globular clusters: individual: M3

1 INTRODUCTION

Nonlinear numerical modeling of classical pulsating stars (Cepheids, RR Lyrae stars) has a long history, which started with the first models of Christy (1964) and culminated in the development of the various pulsation codes used today (Bono & Stellingwerf 1994; Yecko et al. 1998; Smolec & Moskalik 2008a). In the meantime, the most important problems shifted from the driving mechanisms to the mode-selection problem (Stellingwerf 1982; Kolláth et al. 2002). The physical formalism also became more complex, and the role of the convective processes in the outer layers of these stars became one of the main problems (Deupree 1977); for a quick walk-through of the development of the 1D nonlinear radial pulsation codes, we refer to Kovács et al. (2023).

The theoretical description of the 1D convection theory also improved from the first attempts of time-dependent mixing length of Gough (1977) and Unno (1967) to the descriptions of Kuhfuss (1986) and Gehmeyr & Winkler (1992). We suggest Baker (1987) for a good review of the history of these theories.

The availability of running non-linear calculations was greatly enhanced by including the code of Smolec & Moskalik (2008a) into the MESA software package (Paxton et al. 2019) as the RSP module. Meanwhile, other groups used other codes to successfully model Cepheid stars (Marconi et al. 2013a,b, 2015; Keller & Wood

2006). The availability of these codes allows computing large grids of models, so for example, Das et al. (2021) have investigated convective and metallicity effects on BL Her model grids, while Kurbah et al. (2023) studied phase-dependent Cepheid period-luminosity relations using model grids, with different parameter sets.

The usage of different convective parameter sets is very common in these studies. This is because there is no overall calibration of the convective parameters currently. In the case of the RSP code, there are only prescriptions (Paxton et al. 2019). It is well known that there should be no existing simple parameter set that suits every pulsator due to the limitations of the theory and the vast differences in the stellar structure of different types of stars in the instability strip (Smolec & Moskalik 2008a). Although Kolláth et al. (2002) gave parameter sets for Cepheids and RR Lyrae stars for the Budapest-Florida code (BpF hereafter) (Yecko et al. 1998), most studies in this field did not include stellar parameter dependence of the convective parameters, while there is evidence in the case of the pulsation code of Bono & Stellingwerf (1994) that convective parameters may be affected by effective temperatures (Di Criscienzo et al. 2004).

Recently we have done a calibration for these parameters for the RSP and BpF codes in the case of the RRab stars (Kovács et al. 2023, hereafter Paper I). In our Paper I, we concluded that there is a degeneracy between the scale parameter of the eddy viscosity pressure $\bar{\alpha}_\nu$ and the dissipation efficiency parameter $\bar{\alpha}_d$, which is dependent on the effective temperature. We also showed that a discrepancy arises between the synthetic light and radial velocity (RV) curves around

* E-mail: g.kovacs@astro.elte.hu

Table 1. The used stars from [Jurcsik et al. \(2017\)](#), and the selected input model parameters.

Star ID	Period* [d]	T_{eff}^* [K]	L_{bol}^{**} [L_{\odot}]	M^a [M_{\odot}]	X^b	Z^b
v056	0.329598	7074	44.7 ± 2.8	0.5636	0.76	0.0005
v086	0.292656	7348	46.2 ± 2.5	0.58154	0.71	0.0005
v097	0.334997	7108	47.7 ± 2.8	0.58339	0.75	0.0006
v107	0.309026	7259	47.4 ± 2.7	0.58881	0.72	0.0006

*: directly adopted from [Jurcsik et al. \(2017\)](#), error is ± 50 K

** : calculated from mean magnitudes of [Jurcsik et al. \(2015\)](#)

^a: calculated from LNA model interpolation, error is $\pm 0.1 M_{\odot}$

^b: derived from the non-linear fits, X , Z errors are ± 0.03 and ± 0.0001 respectively

the blue edge of the instability strip. In the current work, we extend this effort towards RRc stars in an attempt to find a general RR Lyrae parameter set (if such exists), which would help any large-scale modeling efforts requiring extensive model grid computations and will also provide a way into the transition applying multidimensional codes.

2 OBSERVATIONAL DATA

Albeit radial velocity and multi-band light-curve can be fitted with pulsation models simultaneously to derive stellar parameters ([Di Fabrizio et al. 2002](#); [Natale et al. 2008](#); [Marconi et al. 2013b,a, 2015](#)), this approach includes further assumptions regarding the atmosphere of the star which is not modeled by these codes ([Paper I](#)), while using only radial velocity curves we can study the dynamical structure more thoroughly. For this reason, we use only RV curves of [Jurcsik et al. \(2017\)](#) for calibration and V light curves from [Jurcsik et al. \(2015\)](#) only for comparison. We use these data of selected first overtone RR Lyrae stars from the M3 globular cluster based on their RV curve coverage ([Paper I](#)). We use the cleaned and equidistantly re-sampled RV curves calculated from the Hectoshelle@MMT ([Szentgyorgyi et al. 2011](#)) measurements with 1 km/s errors; we also show light curves for comparison, which were measured simultaneously with the Hectoshelle@MMT measurements with the 60/90 Schmidt telescope at Konkoly Observatory ([Jurcsik et al. 2015](#)).

The value of the projection factor (the multiplier factor which connects the measured radial velocities to the actual pulsating velocities of the star and has a value between 1.0 and 1.5) is central in evaluating the radial velocity curves. There is an ongoing debate about whether this p-factor has a period dependence or not ([Molinaro et al. 2012](#); [Marconi et al. 2013a](#); [Trahin et al. 2021](#), and references therein), which can be caused by structural differences among Cepheids, but among RR Lyrae stars the intrinsic stellar parameters span a much smaller parameter range. In this regard, we choose the value of p-factor to $p = 1.34 \pm 0.07$, the same as in [Paper I](#), and consider the uncertainty of the factor in the error propagation of the convective parameters.

We derived the measured stellar parameters in the same way as in [Paper I](#). We have used bolometric corrections of [Torres \(2010\)](#), interstellar cluster reddening from [Schlafly & Finkbeiner \(2011\)](#), and the Baade-Wesselink distances from [Jurcsik et al. \(2017\)](#) to determine the bolometric luminosities of the stars.

Table 2. Parameters of the $\bar{\alpha}_v$ - $\bar{\alpha}_d$ regression: $\bar{\alpha}_d = a + b\bar{\alpha}_v$.

Star	BpF			RSP		
	a	b	R^2	a	b	R^2
v056	-16.35	381.65	0.9661	0.16886	61.3950	0.9645
v086	-24.59	802.76	0.8682	0.22024	130.582	0.9590
v097	-23.59	374.39	0.9475	0.85470	58.4948	0.9698
v107	-14.01	532.11	0.8649	1.43412	87.7540	0.9896

3 MODELS AND THE FITTING METHOD

We aim at determining the eight convective parameters of the non-linear radial pulsation models ([Gehmeyr & Winkler 1992](#); [Kuhfuss 1986](#)) from radial velocity observations in the case of RRc stars in a similar way as it has been recently done for RRab stars in [Paper I](#).

We use the Budapest-Florida code ([Yecko et al. 1998](#)) and the MESA Radial Stellar Pulsation module ([Paxton et al. 2019](#)) for the convective parameter fitting. These two codes are very similar to each other; their main difference is the handling of negative buoyancy effects ([Paper I](#)). For a one-to-one comparison, see our [Paper I](#) and also the original papers of [Yecko et al. \(1998\)](#) and [Smolec & Moskalik \(2008a\)](#).

These types of models have 5 input parameters intrinsic to the star: the stellar mass (M), the bolometric luminosity (L), the effective temperature (T_{eff}), the hydrogen (X) and a metal mass fraction (Z). Some of these parameters are directly measurable (L, T_{eff}), while others can be determined indirectly by the models. As in [Paper I](#), we determine the pulsating mass by interpolating the period from linear models and X and Z by finding the best-fit values from non-linear calculations.

Our fitting procedure remains unchanged from [Kovács et al. \(2023\)](#). Briefly, it means that we run model grids for the dissipation efficiency $\bar{\alpha}_d$ and eddy viscosity parameter $\bar{\alpha}_v$, as these two parameters have the largest effect on the observed RV curves, and they are also degenerate ([Kovács et al. 2023](#)). The turbulent source ($\bar{\alpha}_s$) and convective flux ($\bar{\alpha}_c$) parameters have stronger effects on the synthetic RV and LC curves of first overtones, hence instead of independent fitting (as in [Paper I](#)) we fit these parameters together.

We are fitting the full radial velocity (RV) curve (in contrast with [Paper I](#), where minimum phase was omitted), which weakens the overall fit but helps to avoid nonphysical artificially strong dissipation fronts in the models, that would cause very strong secondary light curve features e.g. flare-like spikes.

4 RESULTS

The RRc stars show a similar degeneracy between the dissipation ($\bar{\alpha}_d$) and eddy viscosity ($\bar{\alpha}_v$) parameters as was observed in the case of RRab stars ([Kovács et al. 2023](#)) (see [Fig. 1](#)), but the regression parameters have a different correlation with the effective temperature which is shown in [Figs. 2. and 3](#). We show our best-fit RV curves alongside the light curves as a reference in [Fig. 4](#). We see good agreement in the amplitudes, albeit secondary light curve features are too large in some cases, especially in the BpF code, which can be attributed to the sensitivity of the features to the underlying convection models ([Marconi 2017](#)).

In addition to the known effects ([Paper I](#)) of $\bar{\alpha}_v$ and $\bar{\alpha}_d$, we found that the convective flux ($\bar{\alpha}_c$) and source parameters ($\bar{\alpha}_s$) have stronger effects on the first overtone stars, and we found that on a $\bar{\alpha}_c - \bar{\alpha}_s$ grid, the parameters show a degeneracy of hyperbolic shape, for each star. We can see this also by recalculating this grid for the RRab stars

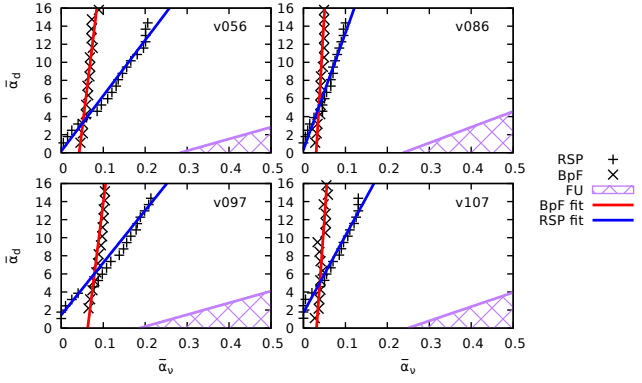


Figure 1. Correlation between the eddy viscosity ($\bar{\alpha}_v$, x axis) and turbulent dissipation ($\bar{\alpha}_d$, y axis) parameters. Crosses are the best fits of the BpF code, while plus signs are the best fits of the RSP code, and the red and blue lines are the regression lines for the BpF and RSP respectively. The purple crossed area refers to parameters where the pulsation switches to fundamental mode and is damped.

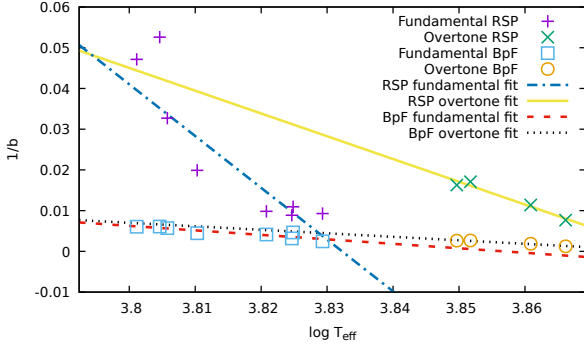


Figure 2. Correlation between the effective temperature and the slope of the $\alpha_v(\alpha_d)$ functions for both pulsation modes and codes as well. Every point is the $1/b$ value from Table 2 corresponding to a single star and one of the codes (see legend), while the x axis is the logarithm of the effective temperature. The fundamental mode values are from Paper I. The lines are the correlations corresponding to the pulsation codes and modes. One can see that the RRab and RRc correlations differ for both codes, but it is more prominent in the case of the RSP code.

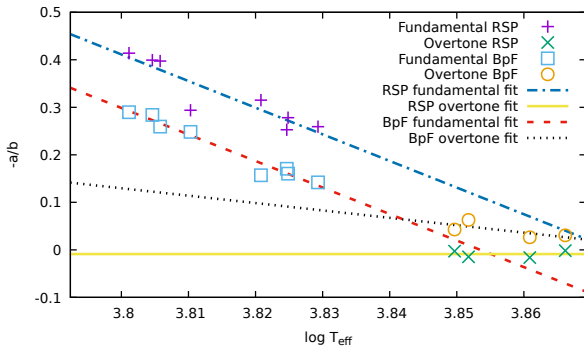


Figure 3. Same as Fig. 2. but for the interception ($-a/b$ from Table 2.) of the $\alpha_v(\alpha_d)$ functions.

Table 3. Convective flux parameters for the two codes choosing $\bar{\alpha}_c = \bar{\alpha}_s$

Star	RSP	BpF
v086	0.2572 ± 0.02	0.1418 ± 0.03
v097	0.4361 ± 0.02	0.1880 ± 0.05
v056	0.3591 ± 0.04	0.2093 ± 0.03
v107	0.3716 ± 0.08	0.1658 ± 0.03

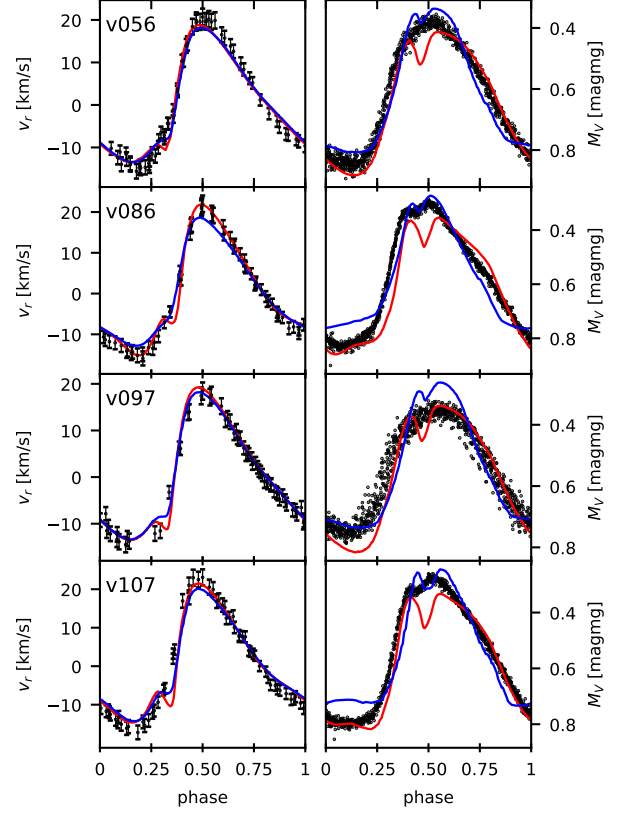


Figure 4. Best fitting results for the studied M3 RRc stars. Left panel: radial velocities, right panel: absolute V magnitude. BpF results marked with the red line, RSP is the blue line. Black dots mark observations.

from Paper I. This hyperbole has an interception with the $\bar{\alpha}_s = \bar{\alpha}_c$ line, so we can further reduce the number of free parameters by one.

We present the details of these results for both codes separately below.

4.1 BpF results

In the case of the BpF the $\bar{\alpha}_d - \bar{\alpha}_v - T_{\text{eff}}$ correlation is the following:

$$\bar{\alpha}_v = (-1.5568 \pm 1) \log T_{\text{eff}} - (0.0859 \pm 0.01) \bar{\alpha} \log T_{\text{eff}} + (0.3336 \pm 0.04) \bar{\alpha}_d + (6.0454 \pm 3.92) \quad (1)$$

The rms of the fit is 0.010.

The $\bar{\alpha}_c = \bar{\alpha}_s$ parameters (3) show a correlation with temperature ($R^2 = 0.9568$), while RRab parameters don't show this feature. But due to the large errors and the low number of points, one can use a generally constant value of 0.17 ± 0.02 for both parameters, which is within the errors of the previous values of RRab stars. $\bar{\alpha}_r$ and $\bar{\alpha}_p$ have little effect on actual RV and light curves.

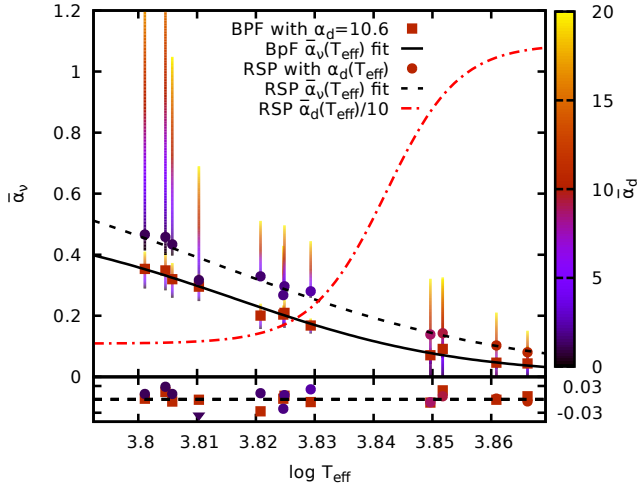


Figure 5. General $\bar{\alpha}_v(T_{\text{eff}})$ functions fitted to the RR Lyrae stars. Colored lines show the individual $\bar{\alpha}_v$ ($\bar{\alpha}_d$) functions in the $\log T_{\text{eff}} - \bar{\alpha}_v$ plane ($\bar{\alpha}_d \in [0, 20]$), the color denotes the $\bar{\alpha}_d$ value. Filled squares: BpF values for $\bar{\alpha}_d = 10.8$, black solid curve: fitted sigmoid of the BpF. Filled circles: results of the RSP code. Here $\bar{\alpha}_d$ also changes to reach the best-fit value, which is shown by the red dashed-dotted curve (for better visibility, we show $\bar{\alpha}_d/10$). The black dashed curve is the fitted sigmoid to the RSP values. The lower panel show residuals where the color codes are as the $\bar{\alpha}_d$ value of the point and the triangle shows outlier points.

4.2 RSP results

In the case of the RSP code, the correlation of the $\bar{\alpha}_v - \bar{\alpha}_d - T_{\text{eff}}$ is as follows:

$$\bar{\alpha}_v = (-0.5591 \pm 0.078)\bar{\alpha}_d \log T_{\text{eff}} + (2.16595 \pm 0.03)\bar{\alpha}_d - (0.0088 \pm 0.0038) \quad (2)$$

with an rms of 0.027.

The $\bar{\alpha}_c = \bar{\alpha}_s$ parameters are weakly correlated ($R^2 \approx 0.5$) and differ from the RRab case. The changes introduced on the RV curves are small while having stronger effects on the light curves. Because of this, we also considered the light curve shape in the fitting process, and this way, the mean $\bar{\alpha}_c = 0.35 \pm 0.06$, which is greater than the RRab value of $\bar{\alpha}_c = 0.30 \pm 0.07$ but they match within the errorbars. Because of this, we can suggest a general value of $\bar{\alpha}_c = \bar{\alpha}_s = 0.32 \pm 0.07$. The $\bar{\alpha}_t$ (turbulent flux) parameter has a small effect, and its best value is around 0.61.

4.3 General RR Lyrae parameter set

We also derived a general set for the eddy viscosity ($\bar{\alpha}_v$) and dissipation ($\bar{\alpha}_d$) parameters, which can be seen in Fig. 5. For this purpose, we have chosen the logistic function in the form of:

$$f(T_{\text{eff}}) = \frac{a}{\exp[b(T_{\text{eff}} - c)] + 1} + d \quad (3)$$

This function can quickly converge to d and $a + d$, which is ideal for avoiding unphysical parameters (negative and too high $\bar{\alpha}$ -s).

In the BpF case, we could get a good fit with $\bar{\alpha}_d = 10.8$, while in the case of the RSP code, it was necessary for $\bar{\alpha}_d$ to change with a logistic function, too. We present these parameters in Table 4.

Table 4. Parameters of function Eq. 3, in different cases.

Case	a	b	c	d	rms
BpF $\bar{\alpha}_v$	0.526 ± 0.008	0.0033 ± 0.0002	6525 ± 10	0.005	0.015
RSP $\bar{\alpha}_v$	0.775 ± 0.02	0.0024 ± 0.0002	6444 ± 10	0.01	0.02
RSP $\bar{\alpha}_d$	9.7979	-0.01	6950	1.089	N/A

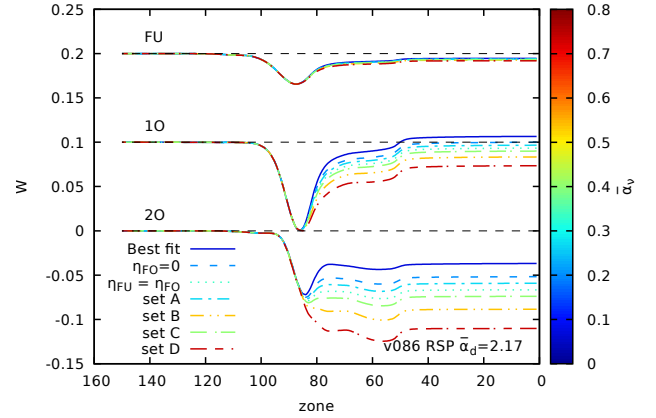


Figure 6. Cumulative work integrals for different $\bar{\alpha}_v$ parameters in the case of the v086 RRC star calculated by the RSP code, shifted to fit on a single figure. Color code shows the value of the $\bar{\alpha}_v$ parameter. From top to bottom: fundamental mode, 1st overtone, 2nd overtone. Black dashed line corresponds to zero.

5 DISCUSSION

The fact that we arrived at different parameter sets for different pulsational modes can be understood since the convective processes influence mode selection, and in turn, the selected mode affects the stellar structure and transport processes. In practice, this means that the $\bar{\alpha}$ parameters depend not only on the physical parameters of the matter but also on the flow structure. We can see an example of this interaction in Fig. 7. Here we can see that in the case of the RRc stars, the flow itself helps to separate the two convective regions, while in the RRab case, the convective zones are connected independently from the temperature. The exact interaction between pulsation and convection is still a research subject, and it can be done using multi-dimensional pulsation codes (Kupka & Muthsam 2017; Mundprecht et al. 2015; Geroux & Deupree 2015).

As the mode selection problem can lead to disjoint sets of structural properties between pulsators (Szabó et al. 2004), this different response to the parameters is understandable but also may question the validity of the mode-selection surveys. In spite of this, the BpF code has more restricted parameter space, which strengthens these studies, while in the case of the RSP code, set B and D are in the purple region of Fig. 1, which means this parameter sets can lead to misleading results. Moreover, higher temperature RRc stars can be rendered pulsationally stable (non-pulsating) with parameter sets A and B as well. In Figure 6 we can see the linear cumulative work integrals¹ of the star V086 ($T_{\text{eff}} = 7348$ K). We can see that the effect of the convective parameters increases for higher overtones. Altogether, we can assume that some features like the fundamental

¹ The cumulative sum of the amount of work done by the sum of the pressure terms during one pulsational cycle calculated over the zones

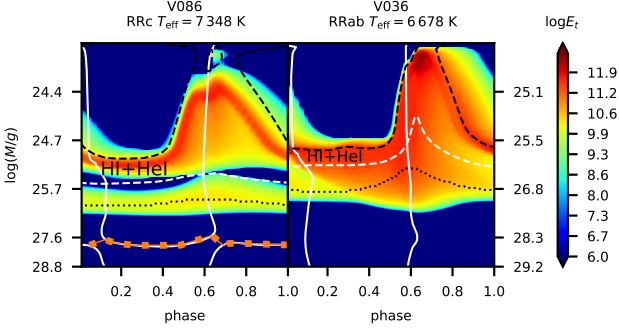


Figure 7. Changing the turbulent energy profile throughout the pulsations in an RRc (left panel, $T_{\text{eff}} = 7348$ K) and in an RRab model (right panel, $T_{\text{eff}} = 6678$ K.) star calculated by the RSP code. X axis is the pulsation phase, Y axis is the logarithm of the mass coordinate from the surface. Color denotes the strength of the turbulent energy. White lines are the zero velocity isocurves. HI and HeI partial ionization zones overlaps, the boundaries of this overlapped zone are denoted by black (outer boundary) and white (inner boundary) dashed curves. The HeII zone is narrow, we show it by the black dotted curve. The position of the nodal line in the RRc star is denoted by the orange dotted curve. Note that due to the phase differences the nodal line is moving and also briefly disappearing in certain phases, which is shown by the fact that the zero velocity curves are not contacting each other. RRc stars have different convective patterns: the HeII zone’s convective region is separated from the HI region. In the case of the RRab stars, the two regions are merged. Towards lower temperatures, e_t is also higher.

blue edge (Szabó et al. 2004) or the period-doubling phenomena (Smolec 2016) are probably more robust, while other features like RRd regions (Szabó et al. 2004; Smolec & Moskalik 2008b) are more sensitive to the convective parameters.

The joint RR Lyrae parameter set has been chosen and calibrated to describe stars in the given temperature range $T \in [6000; 7500]$ K, and due to the sigmoid functions, it has believable constraints outside of this range. Further work on calibration to Cepheid stars may reveal more details regarding the connection between the parameter space and intrinsic stellar parameters. The light and RV curves are insensitive to the turbulent flux and pressure ($\bar{\alpha}_t, \bar{\alpha}_p$) parameters, making some features smoother. These parameters have larger roles in mode selection, so they can be better calibrated by e.g., fundamental blue edge or other features.

6 CONCLUSIONS

We continued our previous work (Kovács et al. 2023) on scrutinizing the convective parameter space of the 1D non-linear radial stellar pulsation codes, the Budapest-Florida and MESA Radial Stellar Pulsations. We used high-precision radial velocity measurements of four first overtone RR Lyrae stars from globular cluster M3 measured by Jurcsik et al. (2017).

We fitted the convective parameters to these RV curves and found degeneracies between the parameters similar but also different to the RRab case. This different nature of the parameters can be interpreted as the effect of the different flow structures of the modes. Nevertheless, the two (RRab and RRc) parameter sets can be approximated by sigmoid functions to reach a general RR Lyrae parameter set, which can be used for survey-like studies and also for comparison with multi-dimensional models. Some parameters have little effect on the observables, but mode-selection features can calibrate them.

Table 5. Recommended parameter sets for RRab (Paper I), RRc stars, and generally RR Lyrae stars (this paper).

	$\bar{\alpha}$	RRab set	RRc set	RR Lyr set
RSP	$\bar{\alpha}_\Lambda$	1.5	1.5	1.5
	$\bar{\alpha}_\nu$	$-8.65 \log T_{\text{eff}} + 33.38$	$-6.085 \log T_{\text{eff}} + 23.564$	Table 4.
	$\bar{\alpha}_t$	0.24 ± 0.03	0.61 ± 0.05	0.61 ± 0.05
	$\bar{\alpha}_p$	2/3	2/3	2/3
	$\bar{\alpha}_d$	$8/3\sqrt{2/3}$	10.883	Table 4.
	$\bar{\alpha}_s$	0.31 ± 0.07	0.35 ± 0.06	0.32 ± 0.06
	$\bar{\alpha}_c$	0.27 ± 0.03	0.35 ± 0.06	0.32 ± 0.06
	$\bar{\alpha}_r$	0	0	0
	T_{eff}	< 7227 K	< 7455 K	N/A
	BpF	$\bar{\alpha}_\Lambda$	1.5	1.5
$\bar{\alpha}_\nu$		$-6.77 \log T_{\text{eff}} + 26.09$	$-2.467 \log T_{\text{eff}} + 9.581$	Table 4.
$\bar{\alpha}_t$		0.2733	0.2733	0.2733
$\bar{\alpha}_p$		2/3	2/3	2/3
$\bar{\alpha}_d$		10.6	10.6	10.6
$\bar{\alpha}_s$		0.22 ± 0.08	0.17 ± 0.02	0.17
$\bar{\alpha}_c$		0.17 ± 0.02	0.17 ± 0.02	0.17
$\bar{\alpha}_r$		0	0	0
T_{eff}		< 7141 K	< 7650 K	N/A

Our final results on these temperature-dependent parameter sets can be found in Table 5.

We also found that the standard four-parameter set of the RSP code (Paxton et al. 2019) is inadequate to describe some of the RRc stars as they damp pulsations, while in some cases, sets B and D interfere with the mode selection process. We emphasize the need for more studies in this direction and warn against using parameter sets without sanity checks.

Numerical simulations in 2 and 3 dimensions are the next logical step in pulsation modeling. Our results give further basis to 1D-3D model comparisons (e.g. Mundprecht et al. 2015) by providing observationally calibrated parameters.

ACKNOWLEDGEMENTS

This project has been supported by the Lendület Program of the Hungarian Academy of Sciences, project No. LP2018-7/2022, the ‘SeismoLab’ KKP-137523 Élvonal, OTKA projects K-129249 and NN-129075, as well as the MW-Gaia COST Action (CA18104).

On behalf of Project ‘Hydrodynamical modeling of classical pulsating variables with SPHERLS’ we are grateful for the usage of ELKH Cloud (see Héder et al. 2022, <https://science-cloud.hu/>) which helped us achieve the results published in this paper.

DATA AVAILABILITY

The observations used in this work are publicly available from the online material of Jurcsik et al. (2017), and the RSP numerical code is also available publicly as part of the MESA software (Paxton et al. 2019).

REFERENCES

- Baker N. H., 1987, in Hillebrandt W., Meyer-Hofmeister E., Thomas H. C., Kippenhahn R., eds, Physical Processes in Comets, Stars and Active Galaxies. pp 105–124
- Bono G., Stellingwerf R. F., 1994, *ApJS*, **93**, 233

- Christy R. F., 1964, *Reviews of Modern Physics*, **36**, 555
- Das S., Kanbur S. M., Smolec R., Bhardwaj A., Singh H. P., Rejkuba M., 2021, *MNRAS*, **501**, 875
- Deupree R. G., 1977, *ApJ*, **211**, 509
- Di Criscienzo M., Marconi M., Caputo F., 2004, *Mem. Soc. Astron. Italiana*, **75**, 190
- Di Fabrizio L., et al., 2002, *MNRAS*, **336**, 841
- Gehmeyr M., Winkler K. H. A., 1992, *A&A*, **253**, 92
- Geroux C. M., Deupree R. G., 2015, *ApJ*, **800**, 35
- Gough D. O., 1977, *ApJ*, **214**, 196
- Héder M., et al., 2022, *Információs Társadalom*, **22**, 128
- Jurcsik J., et al., 2015, *ApJS*, **219**, 25
- Jurcsik J., et al., 2017, *MNRAS*, **468**, 1317
- Keller S. C., Wood P. R., 2006, *ApJ*, **642**, 834
- Kolláth Z., Buchler J. R., Szabó R., Csabry Z., 2002, *A&A*, **385**, 932
- Kovács G. B., Nuspl J., Szabó R., 2023, *MNRAS*, **521**, 4878
- Kuhfuss R., 1986, *A&A*, **160**, 116
- Kupka F., Muthsam H. J., 2017, *Living Reviews in Computational Astrophysics*, **3**, 1
- Kurbah K., Deb S., Kanbur S. M., Das S., Deka M., Bhardwaj A., Randall H. R., Kalici S., 2023, *MNRAS*, **521**, 6034
- Marconi M., 2017, in *European Physical Journal Web of Conferences*. p. 06001, doi:10.1051/epjconf/201715206001
- Marconi M., Molinaro R., Ripepi V., Musella I., Brocato E., 2013a, *MNRAS*, **428**, 2185
- Marconi M., et al., 2013b, *ApJ*, **768**, L6
- Marconi M., et al., 2015, *ApJ*, **808**, 50
- Molinaro R., et al., 2012, *ApJ*, **748**, 69
- Mundprecht E., Muthsam H. J., Kupka F., 2015, *MNRAS*, **449**, 2539
- Natale G., Marconi M., Bono G., 2008, *ApJ*, **674**, L93
- Paxton B., et al., 2019, *The Astrophysical Journal Supplement Series*, **243**, 10
- Schlafly E. F., Finkbeiner D. P., 2011, *ApJ*, **737**, 103
- Smolec R., 2016, *MNRAS*, **456**, 3475
- Smolec R., Moskalik P., 2008a, *ActAA*, **58**, 193
- Smolec R., Moskalik P., 2008b, *Acta Astron.*, **58**, 233
- Stellingwerf R. F., 1982, *ApJ*, **262**, 330
- Szabó R., Kolláth Z., Buchler J. R., 2004, *A&A*, **425**, 627
- Szentgyorgyi A., et al., 2011, *PASP*, **123**, 1188
- Torres G., 2010, *The Astronomical Journal*, **140**, 1158
- Trahin B., Breuval L., Kervella P., Mérand A., Nardetto N., Gallenne A., Hocdé V., Gieren W., 2021, *A&A*, **656**, A102
- Unno W., 1967, *PASJ*, **19**, 140
- Yecko P. A., Kollath Z., Buchler J. R., 1998, *AAP*, **336**, 553

This paper has been typeset from a $\text{\TeX}/\text{\LaTeX}$ file prepared by the author.